

### Remarks

Further and favorable reconsideration is respectfully requested in view of the foregoing amendments and following remarks.

### Interview Summary

Initially, Applicants express their appreciation for the courtesy of a personal interview granted to their attorney by Examiner Hoffmann on August 25, 2005, the results of which are summarized in the Interview Summary Form.

During the interview, Applicants' attorney noted that there is an error at page 3, line 2 of the Response filed April 20, 2005, which states that the magnetic susceptibility of alumina is about  $-4 \times 10^6$  emu/cm<sup>3</sup> referring to a Nature publication. The correct magnetic susceptibility of alumina is about  $-4 \times 10^{-6}$  emu/cm<sup>3</sup>, as shown by the attached copy of Rao et al., Current Science, No. 3, March 1953, pages 72-73. The previously cited Nature publication is irrelevant.

One of the exhibits shown to the Examiner during the interview was a table of magnetic susceptibilities (discussed below), which shows magnetic susceptibilities in units of cm<sup>3</sup> mol<sup>-1</sup> and emu mol<sup>-1</sup>, which Applicants' attorney indicated were equivalent units. The Examiner requested proof of the equivalence of these units. This will be discussed below.

The Examiner also requested proof of the statement in the paragraph bridging pages 2 and 3 of the Response filed April 20, 2005.

Applicants' attorney presented a proposal for amending claim 1, which the Examiner suggested be modified to use appropriate Markush language. Amended claim 1 as set forth above includes the Examiner's suggested changes.

### Amendments

Claim 1 has been amended to incorporate the subject matter of claim 3, while deleting reference to the non-ferromagnetic powder having a not cubic system crystal structure. As a result, claims 2 and 3 have been cancelled, and claims 12 and 13 have been amended to delete the term "non-ferromagnetic".

Applicants respectfully submit that these amendments should be entered even though they are being submitted after a final rejection, since the effect of the amendments is to place claim 3 in independent form. Since the Examiner has already examined claim 3, entry of the amendments should not require any further consideration and/or search of the prior art.

#### Response to Rejections

The patentability of the presently claimed invention over the disclosures of the references relied upon by the Examiner in rejecting the claims will be apparent upon consideration of the following remarks.

Initially, the rejection of claim 1 under 35 U.S.C. §102(b) as being anticipated by Topchiashvili et al., as well as the rejection of claim 13 under 35 U.S.C. §103(a) as being unpatentable over this reference, have been rendered moot in view of the claim amendments, since claim 3, which is not subject to either of these rejections, has been incorporated into claim 1.

The rejection of claim 3 under 35 U.S.C. §103(a) as being unpatentable over Topchiashvili et al. in view of Wei et al., as well as the rejection of this claim under 35 U.S.C. §103(a) as being unpatentable over Topchiaschvili et al. in view of Takagi et al., are respectfully traversed.

In the prior Office Action, to which the Examiner refers in the current Office Action, the Examiner acknowledges that Topchiaschvili et al. do not disclose the ceramics of claim 3 but states that it is clear from column 7, lines 17-29 that the method encompasses materials other than the specific ceramics disclosed. But this disclosure at column 7, lines 17-29 of Topchiaschvili et al. does not include any suggestion to those of ordinary skill in the art of any particular ceramics which could be used in place of the  $\text{YBa}_2\text{Cu}_3\text{O}_{7-x}$  or  $\text{Bi}_2\text{Sr}_2\text{Ca}_2\text{Cu}_3\text{O}_{10}$  ceramics of Topchiaschvili et al. Rather, the disclosure at column 7, lines 17-29 represents language typically inserted into patent applications by the patent drafter in an attempt to obtain as broad as possible coverage for the patent claims. This disclosure certainly would not suggest to the art-skilled that any other particular ceramics could be used in the Topchiaschvili et al. method.

The Wei et al. and Takagi et al. references both disclose sintered alumina particles. However, neither of these references has any mention whatsoever of treating the alumina particles in a magnetic field. Nevertheless, the Examiner takes the position that it would be obvious to apply the Topchiaschvili et al. process to alumina, for the advantages of the alumina products or to solve the known alumina problem. However, Applicants respectfully submit that one of ordinary skill in the art would not be motivated to do as the Examiner suggests, because the ceramics of Topchiaschvili et al. (e.g.  $\text{YBa}_2\text{Cu}_3\text{O}_{7-x}$ ) are treated in a magnetic field for orientation of the ceramic particles according to the reference, which is only possible because **the Topchiaschvili et al. ceramics have magnetic susceptibilities which render them susceptible to magnetic orientation, whereas the alumina ceramics of Wei et al. and Takagi et al. have magnetic susceptibilities which do not render them susceptible to magnetic orientation.**

Applicants firmly believe that it is unforeseen that the powders recited in amended claim 1 can be oriented in a magnetic field because it has been thought that the magnetic susceptibility of these powders can be disregarded in general.

The attached table, presented to the Examiner during the interview, shows the magnetic susceptibility of materials in amended claim 1. [Applicants could not find a report of the magnetic susceptibility of aluminum nitride and hydroxyapatite.] This means that the magnetic susceptibility of these materials can be disregarded, and that there would have been no interest in the magnetic characteristics of these materials. As to a composite mixture, Applicants think that they need not show the magnetic susceptibility of a composite mixture since each material of the mixture is able to be oriented (rotated) by the magnetic field.

The attached table of magnetic susceptibilities refers to the CRC Handbook of Chemistry and Physics, and Physical Review B 39, 6594-6599 as references for the magnetic susceptibilities of the materials recited in the table. Copies of these references are enclosed.

The attached table has magnetic susceptibilities in units of  $\text{cm}^3\text{mol}^{-1}$  as well as units of  $\text{emu mol}^{-1}$ . During the interview, Applicants' attorney indicated that these units are equivalent to each other, and the Examiner requested proof of this. Such proof is

submitted herewith, as a copy of “CHRONOLOGICAL SCIENTIFIC for 2005”, pages 412-413, together with an English translation thereof.

It is apparent from the attached table that the magnetic susceptibility of the ceramic of Topchiaschvili et al. is about 100 times greater than the magnetic susceptibility of the ceramics used in the presently claimed invention, in view of which Applicants respectfully submit that one of ordinary skill in the art would not attempt to orient the ceramic particles of the present invention in a magnetic field to achieve magnetic orientation as in Topchiaschvili et al.

Also in support of this argument, Applicants note that it is an incontrovertible fact that the alumina of the Wei et al. and Takagi et al. references is recognized as a nonmagnetic material, as illustrated by, for example, U.S. Patent Application Publication No. 20050083606, and can be used as a nonmagnetic material in various fields. Thus, paragraph [0013] of the US ‘606 publication refers to “. . . a nonmagnetic material such as alumina . . .”

For these reasons, Applicants take the position that one of ordinary skill in the art would not combine the references in the manner suggested by the Examiner, i.e. by treating the alumina of Wei et al. or Takagi et al. for magnetic orientation according to the process of Topchiashvili et al., because the art-skilled would not expect, with any reasonable degree of certainty, that the relatively much lower magnetic susceptibility of alumina renders it susceptible to magnetic orientation. This is especially true considering the use of alumina as a nonmagnetic material in various fields.

The rejection of claims 1-3 and 12-13 under 35 U.S.C. §103(a) as being unpatentable over Morita et al. is respectfully traversed.

The Examiner takes the position that this reference discloses the use of colloidal alumina and using magnetic fields to form oriented ceramics.

However, the magnetic fields in this reference are **not** applied to the alumina, but rather, are applied to strontium ferrite or barium ferrite, which would of course be susceptible to orientation in a magnetic field. **There is no disclosure in the reference that the alumina is susceptible to orientation in a magnetic field.** This is apparent from comparison of Examples 1 and 2 in the reference which use alumina powder and no magnetic field, with Example 3 in the reference which uses strontium ferrite powder with

application of a magnetic field. As indicated above, those of ordinary skill in the art would not expect that alumina could be oriented in a magnetic field because it has been used in nonmagnetic applications in various fields, and has such a low magnetic susceptibility that the art-skilled would not expect that it could oriented in a magnetic field.

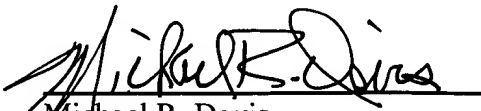
The Response to Arguments section of the Office Action is considered to be moot since it applies to the Topchiashvili et al. reference and claim 1, which has now been amended to incorporate the subject matter of claim 3. The last paragraph on page 5 of the Office Action indicates that the rejection based on Morita et al. is based on the alumina in this reference. But as indicated above, the reference does not disclose or suggest that alumina is or can be treated in a magnetic field to orient the alumina particles. Rather, the magnetic field is applied only to the strontium ferrite powder or barium ferrite powder.

For these reasons, Applicants take the position that the presently claimed invention is clearly patentable over the applied references.

Therefore, in view of the foregoing amendments and remarks, it is submitted that each of the grounds of rejection set forth by the Examiner has been overcome, and that the application is in condition for allowance. Such allowance is solicited.

Respectfully submitted,

Toru SUZUKI et al.

By:   
Michael R. Davis  
Registration No. 25,134  
Attorney for Applicants

MRD/pth  
Washington, D.C. 20006-1021  
Telephone (202) 721-8200  
Facsimile (202) 721-8250  
October 31, 2005

**Table      Magnetic susceptibilities**

<b>Material</b>	<b>Magnetic susceptibilities</b>	<b>Reference</b>
<b>Al<sub>2</sub>O<sub>3</sub></b>	<b>-37 x 10<sup>-6</sup> cm<sup>3</sup> mol<sup>-1</sup></b>	<b>CRC Handbook of Chemistry and Physics</b>
<b>TiO<sub>2</sub></b>	<b>5.9 x 10<sup>-6</sup> cm<sup>3</sup> mol<sup>-1</sup></b>	
<b>ZrO<sub>2</sub></b>	<b>-13.8 x 10<sup>-6</sup> cm<sup>3</sup> mol<sup>-1</sup></b>	
<b>ZnO</b>	<b>-27.2 x 10<sup>-6</sup> cm<sup>3</sup> mol<sup>-1</sup></b>	
<b>SnO<sub>2</sub></b>	<b>-41 x 10<sup>-6</sup> cm<sup>3</sup> mol<sup>-1</sup></b>	
<b>YBa<sub>2</sub>Cu<sub>3</sub>O<sub>7-x</sub></b>	<b>3.5~6.2 x 10<sup>-4</sup> emu mol<sup>-1</sup> (dependence on the X)</b>	<b>Physical Review B 39, 6594-6599</b>

the force constants  $\mu_{11}$ ,  $\mu_{22}$ ,  $\lambda_{11}$ ,  $\lambda_{22}$  for like molecules. From a discussion of the dispersive and repulsive energies of molecular interaction, it can be shown that

$$\epsilon_{12} r_{12}^6 = 2(\epsilon_{11} \epsilon_{22} r_{11}^6 r_{22}^6)^{1/2} (I_1 I_2)^{1/2} / (I_1 + I_2) \quad (3)$$

$$\mu_{12} = (\mu_{11} \mu_{22})^{1/2} \cdot 2 \cdot (I_1 I_2)^{1/2} / (I_1 + I_2) \quad (4)$$

$$\lambda_{12} = (\lambda_{11} \lambda_{22})^{1/2} (r_{11} / r_{11} r_{22})^{1/2} \cdot 2 (I_1 I_2)^{1/2} / (I_1 + I_2) \quad (5)$$

where  $I_1$ ,  $I_2$  are the ionization potentials. These equations show that the assumptions  $\epsilon_{12} = (\epsilon_{11} \epsilon_{22})^{1/2}$  and  $r_{12} = (r_1 + r_2)/2$  hitherto made by workers in this field have no theoretical justification. Tables I and II show that our equa-

TABLE I

Gas pair	$\epsilon_{12}/k$ Expt.	$\epsilon_{12}/k$ (Eqn. 3)	$\epsilon_{12}/k$ Geom. Mean	$r_{12}(\text{\AA})$ Expt.	$r_{12}(\text{\AA})$ (Eqn. 3)	$r_{12}(\text{\AA})$ Arith. Mean
H <sub>2</sub> -N <sub>2</sub>	46.53	51.42	53.86	3.779	3.795	3.774
H <sub>2</sub> -O <sub>2</sub>	59.81	50.99	60.67	3.154	3.108	3.206
H <sub>2</sub> -A	56.41	58.21	64.47	3.541	3.258	3.196
H <sub>2</sub> -CO	52.02	50.28	57.55	3.714	3.745	3.207
He-A	26.05	27.04	27.45	3.041	3.049	3.002

TABLE II

Gas pair	$\mu_{12} \times 10^{80}$ Expt.	erg. cm. <sup>6</sup> (Eqn. 4)	$\lambda_{12} \times 10^{104}$ Expt.	erg. cm. <sup>12</sup> (Eqn. 5)
H <sub>2</sub> -N <sub>2</sub>	35.4	39.1	4.91	5.43
H <sub>2</sub> -O <sub>2</sub>	24.8	35.5	3.09	3.77
H <sub>2</sub> -A	35.8	37.0	4.15	4.28
H <sub>2</sub> -CO	41.4	40.0	5.99	5.80
He-A	11.6	11.7	0.91	0.89

tions give much better agreement with the experimentally determined values than the hitherto assumed empirical relations.

Using these force constants thus obtained from thermal diffusion and equation (3), the transport coefficients of certain binary gas mixtures have been calculated. It has been found that the agreement between theory and experiment is quite satisfactory, thereby proving the correctness of the force constants determined by us.

Detailed reports are being published elsewhere.

Dept. of Physics, B. N. SRIVASTAVA.  
Lucknow University, M. P. MADAN.  
January 19, 1953.

1. Chapman, S., and Cowling, T. G., *The Mathematical Theory of Non-Uniform Gases* (Cambridge University Press, 1939). 2. Grew, K. E., and Ibbs, T. L. *Thermal Diffusion in Gases* (Cambridge University Press, 1952).

## MAGNETIC STUDY OF SOME FORMS OF CORUNDUM

CORUNDUM (an oxide of aluminium, Al<sub>2</sub>O<sub>3</sub>) is known as white sapphire in its pure form. Admixture of small quantities of chromic oxide imparts a beautiful red colour and the specimen is then well known in gemmology as ruby. Since Cr<sub>2</sub>O<sub>3</sub> is isomorphous with Al<sub>2</sub>O<sub>3</sub>, chromium may be assumed to take the place of aluminium in the crystal. Similarly the blue colour of sapphire is due to the presence of titanium in the form of TiFeO<sub>3</sub>.

The invention of the Verneuil furnace in 1904 has made the production of large quantities of transparent synthetic corundum possible.<sup>1</sup> Several physical properties of these specimens very closely resemble those of the corresponding natural stones. A magnetic study of synthetic and natural forms of ruby and white sapphire was undertaken from this point of view.

The principal magnetic susceptibilities were studied by Krishnan's critical torsion method.<sup>3</sup> The mean specific susceptibilities were obtained with the Curie balance.  $\alpha$ -corundum crystallizes in the rhombohedral division of the hexagonal system.<sup>4</sup> The rhombohedral axis is also the optic axis of the crystal. The values of the specific susceptibility parallel and perpendicular to this axis are tabulated below.\*

	$\chi_{\perp}$	$\chi_{\parallel}$	$(\chi_{\perp} - \chi_{\parallel})$
Synthetic ruby	+0.41	+0.38	0.03
Synthetic white sapphire	-0.21	-0.25	0.04
Natural ruby †	-0.15	-0.20	0.05

The values of the anisotropy were found to be nearly equal. The principal susceptibilities of natural sapphire could not be determined since crystals of suitable size were not available. The magnetic properties of  $\alpha$ -corundum are found to be similar to those of calcite, which is also a negative crystal and which crystallizes in the same division. The principal susceptibilities of the O<sub>3</sub> group (the centres of the oxygens being at the vertices of an equilateral triangle of side 2.3 Å) are found to be -29.1 (normal to the plane) and -34.2 (in the plane) per gram molecule of alumina. The anisotropy is of the same order of magnitude as the values obtained with CO<sub>2</sub> and NO<sub>2</sub> groups.<sup>5</sup>

The results obtained with several specimens showed that the mean specific susceptibilities of synthetic and natural white sapphire (-0.22 and -0.35) were close to the value of -0.376.

obtained by adding the ionic contributions. On the other hand, synthetic ruby was strongly paramagnetic (nearly 0.40) while the specimens of natural ruby of nearly the same red colour were all diamagnetic ( $-0.16$ ). These results are in complete accord with the results of chemical analysis that in synthetic ruby, there is far greater percentage of chromic oxide than in the natural stones.<sup>2</sup> Our calculations give 0.82 per cent. in synthetic ruby and 0.27 per cent. in the best available natural specimens.

Full details will be published in the *Journal of the University of Mysore*.

Central College,  
Bangalore,  
February 17, 1953.

S. RAMACHANDRA RAO.  
M. LEELA.

\* All  $\chi$  values are given in  $10^{-8}$  unit.

† From the richness of colour these were the best stones available with the jewellers.

1. Herbert Smith, *Gemstones*, 1950, p. 276. 2. *Ibid.*, p. 184. 3. Krishnan and Banerjee, *Phil. Trans. Roy. Soc.*, 1935, 234, 267; see also (5), 30. 4. Wyckoff, *The Structure of Crystals*, A.C.S. Monographs, 1931, 254. 5. Nilakantan, *Studies in Crystal Magnetism*, Thesis, Madras, p. 44.

### CONDUCTOMETRIC ESTIMATION OF CERIUM IN DILUTE CERIOUS CHLORIDE AS OXALATE

FOR the quantitative estimation of the rare earths as oxalate, the acidity of the solution requires careful adjustment.<sup>1</sup> Further, the rare-earth oxalates, e.g., that of cerium, are not completely insoluble even in the presence of excess oxalic acid.<sup>2</sup> In view of the success of the conductometric method of estimation, as oxalates of Ca, Ag, Cu, Co, Ni, etc.,<sup>3,4</sup> it was of interest to extend the method to cerium and other rare earths.

Conductometric titration of  $10.0$ ,  $5.0$  and  $3.3 \times 10^{-4}$  M. cerous chloride (Merck's guaranteed extra pure), against  $0.01$  M. ammonium oxalate and oxalic acid (Analar samples), was carried out at  $30 \pm 0.05^\circ \text{C}$ . in a Pyrex conductivity cell with platinum electrodes using a Pye's modified Post Office Box of dial resistance type. Air-free conductivity water was employed for preparing the various solutions. The results obtained are represented in the graph where the conductivity, corrected for dilution, is plotted against the volume of titrant added.

It is seen from the table that the conductometric method of estimation as oxalate, is applicable to cerium in cerous chloride, in dilute

solution. This method is more advantageous than the ordinary chemical methods since in

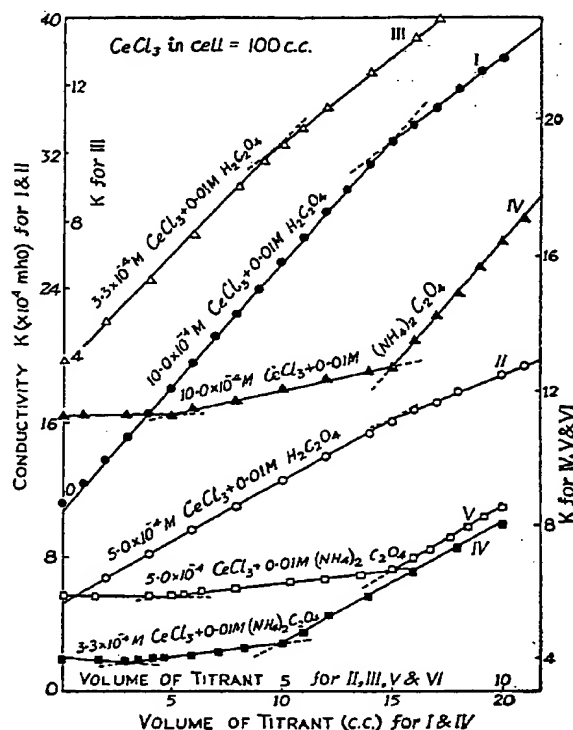
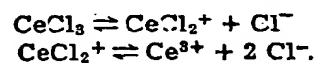


**TABLE**  
Conductometric Estimation of Cerium in Dilute  
Cerous Chloride as Oxalate  
CeCl<sub>3</sub> taken in the cell = 100 c.c.  
Temp.  $30 \pm 0.05^\circ \text{C}$ .

Concn. of CeCl <sub>3</sub> $10^{-4}$ M	Am. oxalate for complete pptn. of Ce as Ce <sub>2</sub> (C <sub>2</sub> O <sub>4</sub> ) <sub>3</sub> c.c.	Observed am. oxalate for complete pptn. c.c.	Oxalic acid for complete pptn. of Ce as Ce <sub>2</sub> (C <sub>2</sub> O <sub>4</sub> ) <sub>3</sub> c.c.	Observed oxalic acid for complete pptn.
10.0	15.00	15.0	15.00	15.0
5.0	7.50	7.5	7.50	7.5
3.3	5.00	5.0	5.00	5.0

large dilution the latter fail.<sup>5</sup> The CeCl<sub>3</sub> — (NH<sub>4</sub>)<sub>2</sub> C<sub>2</sub>O<sub>4</sub> curves exhibit two breaks in every case, when  $\text{Ce}^{3+} : \text{C}_2\text{O}_4^{2-} :: 2 : 1$  and  $2 : 3$  respectively. This might result from two-stage ionisation of cerous chloride, viz.,

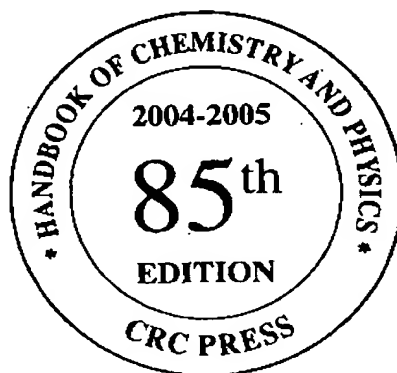


The reactions occurring on gradual addition of ammonium oxalate to cerous-chloride would be:

BEST AVAILABLE COPY

# CRC Handbook of Chemistry and Physics

A Ready-Reference Book of Chemical and Physical Data



Editor-in-Chief

**David R. Lide, Ph.D.**

Former Director, Standard Reference Data  
National Institute of Standards and Technology



CRC Press

Boca Raton London New York Washington, D.C.

## MAGNETIC SUSCEPTIBILITY OF THE ELEMENTS AND INORGANIC COMPOUNDS

When a material is placed in a magnetic field  $H$ , a magnetization (magnetic moment per unit volume)  $M$  is induced in the material which is related to  $H$  by  $M = \kappa H$ , where  $\kappa$  is called the volume susceptibility. Since  $H$  and  $M$  have the same dimensions,  $\kappa$  is dimensionless. A more useful parameter is the molar susceptibility  $\chi_m$ , defined by

$$\chi_m = \kappa V_m = \kappa M/\rho$$

where  $V_m$  is the molar volume of the substance,  $M$  the molar mass, and  $\rho$  the mass density. When the cgs system is used, the customary units for  $\chi_m$  are  $\text{cm}^3 \text{mol}^{-1}$ ; the corresponding SI units are  $\text{m}^3 \text{mol}^{-1}$ .

Substances that have no unpaired electron orbital or spin angular momentum generally have negative values of  $\chi_m$  and are called diamagnetic. Their molar susceptibility varies only slightly with temperature. Substances with unpaired electrons, which are termed paramagnetic, have positive  $\chi_m$  and show a much stronger temperature dependence, varying roughly as  $1/T$ . The net susceptibility of a paramagnetic substance is the sum of the paramagnetic and diamagnetic contributions, but the former almost always dominates.

This table gives values of  $\chi_m$  for the elements and selected inorganic compounds. All values refer to nominal room temperature (285 to 300 K) unless otherwise indicated. When the physical state (s = solid, l = liquid, g = gas, aq = aqueous solution) is not given, the most common crystalline form is understood. An entry of Ferro. indicates a ferromagnetic substance.

Substances are arranged in alphabetical order by the most common name, except that compounds such as hydrides, oxides, and acids are grouped with the parent element (the same ordering used in the table Physical Constants of Inorganic Compounds).

In keeping with customary practice, the molar susceptibility is given here in units appropriate to the cgs system. These values should be multiplied by  $4\pi$  to obtain values for use in SI equations (where the magnetic field strength  $H$  has units of  $\text{A m}^{-1}$ ).

## REFERENCES

1. Landolt-Börnstein, *Numerical Data and Functional Relationships in Science and Technology, New Series*, II/16, *Diamagnetic Susceptibility*, Springer-Verlag, Heidelberg, 1986.
2. Landolt-Börnstein, *Numerical Data and Functional Relationships in Science and Technology, New Series*, III/19, Subvolumes a to i2, *Magnetic Properties of Metals*, Springer-Verlag, Heidelberg, 1986-1992.
3. Landolt-Börnstein, *Numerical Data and Functional Relationships in Science and Technology, New Series*, II/2, II/8, II/10, II/11, and II/12a, *Coordination and Organometallic Transition Metal Compounds*, Springer-Verlag, Heidelberg, 1966-1984.
4. *Tables de Constantes et Données Numérique, Volume 7, Relaxation Paramagnétique*, Masson, Paris, 1957.

Name	Formula	$\chi_m/10^{-6} \text{ cm}^3 \text{mol}^{-1}$	Name	Formula	$\chi_m/10^{-6} \text{ cm}^3 \text{mol}^{-1}$
Aluminum	Al	+16.5	Arsenic (yellow)	As	-23.2
Aluminum trifluoride	AlF <sub>3</sub>	-13.9	Arsine (g)	AsH <sub>3</sub>	-35.2
Aluminum oxide	Al <sub>2</sub> O <sub>3</sub>	-37	Arsenic(III) bromide	AsBr <sub>3</sub>	-106
Aluminum sulfate	Al <sub>2</sub> (SO <sub>4</sub> ) <sub>3</sub>	-93	Arsenic(III) chloride	AsCl <sub>3</sub>	-72.5
Ammonia (g)	NH <sub>3</sub>	-16.3	Arsenic(III) iodide	AsI <sub>3</sub>	-142.2
Ammonia (aq)	NH <sub>3</sub>	-18.3	Arsenic(III) oxide	As <sub>2</sub> O <sub>3</sub>	-30.34
Ammonium acetate	NH <sub>4</sub> C <sub>2</sub> H <sub>3</sub> O <sub>2</sub>	-41.1	Arsenic(III) sulfide	As <sub>2</sub> S <sub>3</sub>	-70
Ammonium bromide	NH <sub>4</sub> Br	-47	Barium	Ba	+20.6
Ammonium carbonate	(NH <sub>4</sub> ) <sub>2</sub> CO <sub>3</sub>	-42.5	Barium bromide	BaBr <sub>2</sub>	-92
Ammonium chlorate	NH <sub>4</sub> ClO <sub>3</sub>	-42.1	Barium bromide dihydrate	BaBr <sub>2</sub> ·2H <sub>2</sub> O	-119.3
Ammonium chloride	NH <sub>4</sub> Cl	-36.7	Barium carbonate	BaCO <sub>3</sub>	-58.9
Ammonium fluoride	NH <sub>4</sub> F	-23	Barium chloride	BaCl <sub>2</sub>	-72.6
Ammonium iodate	NH <sub>4</sub> IO <sub>3</sub>	-62.3	Barium chloride dihydrate	BaCl <sub>2</sub> ·2H <sub>2</sub> O	-100
Ammonium iodide	NH <sub>4</sub> I	-66	Barium fluoride	BaF <sub>2</sub>	-51
Ammonium nitrate	NH <sub>4</sub> NO <sub>3</sub>	-33	Barium hydroxide	Ba(OH) <sub>2</sub>	-53.2
Ammonium sulfate	(NH <sub>4</sub> ) <sub>2</sub> SO <sub>4</sub>	-67	Barium iodate	Ba(IO <sub>3</sub> ) <sub>2</sub>	-122.5
Ammonium thiocyanate	NH <sub>4</sub> SCN	-48.1	Barium iodide	BaI <sub>2</sub>	-124.4
Antimony	Sb	-99	Barium iodide dihydrate	BaI <sub>2</sub> ·2H <sub>2</sub> O	-163
Stibine (g)	SbH <sub>3</sub>	-34.6	Barium nitrate	Ba(NO <sub>3</sub> ) <sub>2</sub>	-66.5
Antimony(III) bromide	SbBr <sub>3</sub>	-111.4	Barium oxide	BaO	-29.1
Antimony(III) chloride	SbCl <sub>3</sub>	-86.7	Barium peroxide	BaO <sub>2</sub>	-40.6
Antimony(III) fluoride	SbF <sub>3</sub>	-46	Barium sulfate	BaSO <sub>4</sub>	-65.8
Antimony(III) iodide	SbI <sub>3</sub>	-147.2	Beryllium	Be	-9.0
Antimony(III) oxide	Sb <sub>2</sub> O <sub>3</sub>	-69.4	Beryllium chloride	BeCl <sub>2</sub>	-26.5
Antimony(III) sulfide	Sb <sub>2</sub> S <sub>3</sub>	-86	Beryllium hydroxide	Be(OH) <sub>2</sub>	-23.1
Antimony(V) chloride	SbCl <sub>5</sub>	-120.5	Beryllium oxide	BeO	-11.9
Argon (g)	Ar	-19.32	Beryllium sulfate	BeSO <sub>4</sub>	-37
Arsenic (gray)	As	-5.6	Bismuth	Bi	-280.1

# MAGNETIC SUSCEPTIBILITY OF THE ELEMENTS AND INORGANIC COMPOUNDS (continued)

Name	Formula	$\chi_m/10^{-6} \text{ cm}^3 \text{ mol}^{-1}$	Name	Formula	$\chi_m/10^{-6} \text{ cm}^3 \text{ mol}^{-1}$
Sroutium peroxide	SrO <sub>2</sub>	-32.3	Tungsten carbide	WC	+10
Sroutium sulfate	SrSO <sub>4</sub>	-57.9	Tungsten(II) chloride	WCl <sub>2</sub>	-25
Sulfur (rhombic)	S	-15.5	Tungsten(IV) oxide	WO <sub>2</sub>	+57
Sulfur (monoclinic)	S	-14.9	Tungsten(IV) sulfide	WS <sub>2</sub>	+5850
Sulfuric acid (l)	H <sub>2</sub> SO <sub>4</sub>	-39	Tungsten(V) bromide	WBr <sub>5</sub>	+270
Sulfur dioxide (g)	SO <sub>2</sub>	-18.2	Tungsten(V) chloride	WCl <sub>5</sub>	+387
Sulfur trioxide (l)	SO <sub>3</sub>	-28.54	Tungsten(VI) chloride	WCl <sub>6</sub>	-71
Sulfur chloride (l)	SSCl <sub>2</sub>	-62.2	Tungsten(VI) fluoride (g)	WF <sub>6</sub>	-53
Sulfur dichloride (l)	SCl <sub>2</sub>	-49.4	Tungsten(VI) oxide	WO <sub>3</sub>	-15.8
Sulfur hexafluoride (g)	SF <sub>6</sub>	-44	Uranium	U	+409
Thionyl chloride (l)	SOCl <sub>2</sub>	-44.3	Uranium(III) bromide	UBr <sub>3</sub>	+4740
Tantalum	Ta	+154	Uranium(III) chloride	UCl <sub>3</sub>	+3460
Tantalum(V) chloride	TaCl <sub>5</sub>	+140	Uranium(III) hydride	UH <sub>3</sub>	+6244
Tantalum(V) oxide	Ta <sub>2</sub> O <sub>5</sub>	-32	Uranium(III) iodide	UI <sub>3</sub>	+4460
Technetium	Tc	+115	Uranium(IV) bromide	UBr <sub>4</sub>	+3530
Tellurium	Te	-38	Uranium(IV) chloride	UCl <sub>4</sub>	+3680
Tellurium dibromide	TeBr <sub>2</sub>	-106	Uranium(IV) fluoride	UF <sub>4</sub>	+3530
Tellurium dichloride	TeCl <sub>2</sub>	-94	Uranium(IV) oxide	UO <sub>2</sub>	+2360
Tellurium hexafluoride (g)	TeF <sub>6</sub>	-66	Uranium(VI) fluoride	UF <sub>6</sub>	+43
Terbium (α)	Tb	+170000	Uranium(VI) oxide	UO <sub>3</sub>	+128
Terbium oxide	Tb <sub>2</sub> O <sub>3</sub>	+78340	Vanadium	V	+285
Thallium	Tl	-50	Vanadium(II) bromide	VBr <sub>2</sub>	+3230
Thallium(I) bromate	TlBrO <sub>3</sub>	-75.9	Vanadium(II) chloride	VCl <sub>2</sub>	+2410
Thallium(I) bromide	TlBr	-63.9	Vanadium(III) bromide	VBr <sub>3</sub>	+2910
Thallium(I) carbonate	Tl <sub>2</sub> CO <sub>3</sub>	-101.6	Vanadium(III) chloride	VCl <sub>3</sub>	+3030
Thallium(I) chlorate	TlClO <sub>3</sub>	-65.5	Vanadium(III) fluoride	VF <sub>3</sub>	+2757
Thallium(I) chloride	TlCl	-57.8	Vanadium(III) oxide	V <sub>2</sub> O <sub>3</sub>	+1976
Thallium(I) chromate	Tl <sub>2</sub> CrO <sub>4</sub>	-39.3	Vanadium(III) sulfide	V <sub>2</sub> S <sub>3</sub>	+1560
Thallium(I) cyanide	TlCN	-49	Vanadium(IV) chloride	VCl <sub>4</sub>	+1215
Thallium(I) fluoride	TlF	-44.4	Vanadium(IV) oxide	VO <sub>2</sub>	+99
Thallium(I) iodate	TlIO <sub>3</sub>	-86.8	Vanadium(V) oxide	V <sub>2</sub> O <sub>5</sub>	+128
Thallium(I) iodide	TlI	-82.2	Water (s, 273 K)	H <sub>2</sub> O	-12.63
Thallium(I) nitrate	TlNO <sub>3</sub>	-56.5	Water (l, 293 K)	H <sub>2</sub> O	-12.96
Thallium(I) nitrite	TlNO <sub>2</sub>	-50.8	Water (l, 373 K)	H <sub>2</sub> O	-13.09
Thallium(I) sulfate	Tl <sub>2</sub> SO <sub>4</sub>	-112.6	Water (g, 373 K)	H <sub>2</sub> O	-13.1
Thallium(I) sulfide	Tl <sub>2</sub> S	-88.8	Xenon (g)	Xe	-45.5
Thorium	Th	+97	Ytterbium (β)	Yb	+67
Thorium(IV) oxide	ThO <sub>2</sub>	-16	Yttrium (α)	Y	+187.7
Thulium	Tm	+24700	Yttrium oxide	Y <sub>2</sub> O <sub>3</sub>	+44.4
Thulium oxide	Tm <sub>2</sub> O <sub>3</sub>	+51444	Yttrium sulfide	Y <sub>2</sub> S <sub>3</sub>	+100
Tin (gray)	Sn	-37.4	Zinc	Zn	-9.15
Tin(II) chloride	SnCl <sub>2</sub>	-69	Zinc carbonate	ZnCO <sub>3</sub>	-34
Tin(II) chloride dihydrate	SnCl <sub>2</sub> ·2H <sub>2</sub> O	-91.4	Zinc chloride	ZnCl <sub>2</sub>	-55.33
Tin(II) oxide	SnO	-19	Zinc cyanide	Zn(CN) <sub>2</sub>	-46
Tin(IV) bromide	SnBr <sub>4</sub>	-149	Zinc fluoride	ZnF <sub>2</sub>	-34.3
Tin(IV) chloride (l)	SnCl <sub>4</sub>	-115	Zinc hydroxide	Zn(OH) <sub>2</sub>	-67
Tin(IV) oxide	SnO <sub>2</sub>	-41	Zinc iodide	ZnI <sub>2</sub>	-108
Titanium	Ti	+151	Zinc oxide	ZnO	-27.2
Titanium(II) bromide	TiBr <sub>2</sub>	+720	Zinc phosphate	Zn <sub>3</sub> (PO <sub>4</sub> ) <sub>2</sub>	-141
Titanium(II) chloride	TiCl <sub>2</sub>	+484	Zinc sulfate	ZnSO <sub>4</sub>	-47.8
Titanium(II) iodide	TiI <sub>2</sub>	+1790	Zinc sulfate monohydrate	ZnSO <sub>4</sub> ·H <sub>2</sub> O	-63
Titanium(II) sulfide	TiS	+432	Zinc sulfate heptahydrate	ZnSO <sub>4</sub> ·7H <sub>2</sub> O	-138
Titanium(III) bromide	TiBr <sub>3</sub>	+660	Zinc sulfide	ZnS	-25
Titanium(III) chloride	TiCl <sub>3</sub>	+1110	Zirconium	Zr	+120
Titanium(III) fluoride	TiF <sub>3</sub>	+1300	Zirconium carbide	ZrC	-26
Titanium(III) oxide	Ti <sub>2</sub> O <sub>3</sub>	+132	Zirconium nitrate	Zr(NO <sub>3</sub> ) <sub>4</sub> ·5H <sub>2</sub> O	-77
Titanium(III) chloride	TiCl <sub>4</sub>	-54	pentahydrate		
Titanium(IV) oxide	TiO <sub>2</sub>	+5.9	Zirconium(IV) oxide	ZrO <sub>2</sub>	-13.8
Tungsten	W	+53			

# Magnetic susceptibility of $\text{YBa}_2\text{Cu}_3\text{O}_{6+x}$ : Effects of spin frustration and correlation

W. E. Farneth, R. S. McLean, and E. M. McCarron III

Central Research and Development Department, E. I. du Pont de Nemours & Co., Wilmington, Delaware 19880-0356

F. Zuo, Y. Lu, and B. R. Patton

Department of Physics, The Ohio State University, Columbus, Ohio 43210-1106

A. J. Epstein

Department of Physics and Department of Chemistry, The Ohio State University, Columbus, Ohio 43210-1106

(Received 1 July 1988; revised manuscript received 9 November 1988)

$\text{YBa}_2\text{Cu}_3\text{O}_{6+x}$  is known to undergo a transition from a magnetic semiconductor to a metallic high-temperature superconductor as the oxygen content is increased from the range  $0.0 \leq x \leq 0.5$  to  $0.5 \leq x \leq 1.0$ . We report here detailed temperature-dependent magnetic-susceptibility studies for  $x$  in the composition range  $0.0 \leq x \leq 1.0$ . For  $0.05 \leq x \leq 0.5$ , the effective moment  $\mu_{\text{eff}}$  decreases with decreasing temperature from 300–160 K, as expected for an antiferromagnet whose Néel temperature is above room temperature. Below 160 K,  $\mu_{\text{eff}}$  increases, reaching a maximum at  $\sim 40$  K then decreases again. The magnitude of this low-temperature peak in  $\mu_{\text{eff}}$  increases with  $x$ , reaches a maximum at  $x=0.35$ , then decreases toward zero. A Monte Carlo simulation method has been used to model the three-dimensional antiferromagnetic ordering of this system as a function of oxygen composition. The calculation reveals the presence of spin frustration as  $x$  increases from 0 through to 0.3 in accord with the increasing number of effective moments at low temperatures. Above  $x=0.3$  a new long-range order (corresponding to a doubling of the magnetic unit cell perpendicular to the planes) is predicted to occur in agreement with the observed magnetic susceptibility and recent neutron-diffraction experiments of Kadowaki *et al.* [Phys. Rev. B 37, 7932 (1988)] and Lynn *et al.* [Phys. Rev. Lett. 60, 2781 (1988)]. Above  $x=0.5$ , relatively few localized moments are observed in the temperature-dependent susceptibility measurement. In the metallic regime the “Pauli susceptibility” is observed to increase approximately linearly with oxygen content. This is in accord with decreasing effects of antiferromagnetic correlation with increasing  $x$ .

## I. INTRODUCTION

The discovery of superconductivity in layered cuprates has stimulated intensive experimental and theoretical study of these and related materials.<sup>1,2</sup> In the  $\text{YBa}_2\text{Cu}_3\text{O}_{6+x}$  system there is an evolution from an antiferromagnetically ordered semiconductor for  $x \leq 0.5$  to a superconducting nonmagnetically ordered system for  $x \geq 0.5$ .<sup>3–7</sup> For  $\text{YBa}_2\text{Cu}_3\text{O}_{6+x}$  with  $x \sim 0$  the magnetic structure consists of a simple antiparallel arrangement of Cu spins both within the Cu-O planes as well as along the tetragonal  $c$  axis, while the oxygen-deficient Cu planes possess no net moment.<sup>4,6</sup> In this system the three-dimensional ordering temperature is high, with  $T_{N1} \sim 450\text{--}500$  K,<sup>3–7</sup> suggesting the presence of large exchange interaction energies. Because of the large separation and resulting anisotropic interactions between the two-dimensional planes containing the Cu spins, two-dimensional magnetic correlations should persist within these planes above  $T_{N1}$ . With increasing  $x$ ,  $T_{N1}$  decreases until no magnetic ordering is observed for  $x \sim 0.4\text{--}0.5$ . Recent neutron-diffraction studies of  $\text{YBa}_2\text{Cu}_3\text{O}_{6+x}$  by Kadowaki *et al.*<sup>8(a)</sup> show that for  $x \approx 0.35$  there is a change in the antiferromagnetic sequencing along the  $c$  axis at  $T_{N2} \sim 40$  K, while for  $x \approx 0.2$  Sato *et al.*<sup>8(b)</sup> have not observed any change in the antiferromagnetic

sequencing down to 5 K. Neutron diffraction studies of  $\text{NdBa}_2\text{Cu}_3\text{O}_{6+x}$  show that changes in antiferromagnetic sequencing are more prominent in this system (perhaps due to greater interaction of the Nd 4f electrons with the surrounding lattice<sup>9</sup>). The magnetic orderings of the 1:2:3 systems are of particular interest because of suggestions that the magnetic interactions are responsible for the high-temperature superconducting pairing in these systems.<sup>10–18</sup>

We report here the results of an extensive study of the temperature ( $T$ ) dependence of the susceptibility ( $\chi$ ) of  $\text{YBa}_2\text{Cu}_3\text{O}_{6+x}$  for  $0.0 \leq x \leq 1.0$ . For  $x \sim 0$ ,  $\chi(T)$  is in agreement with simple antiferromagnetic sequencing of the spins with  $T_{N1} \geq 320$  K, though there is a small increase in  $\chi$  at low  $T$ . With increasing  $x$  this excess susceptibility is more pronounced, reaching a maximum for  $x \sim 0.37$ , and decreasing substantially as  $x$  approaches 0.5. The  $T$ -dependent effective moment  $\mu_{\text{eff}} [=p\mu_B]$ , where  $p \equiv 2.83(\chi T)^{1/2}$  for  $\chi$  in emu/mole  $\text{YBa}_2\text{Cu}_3\text{O}_{6+x}$  and  $T$  in degrees Kelvin] increases with  $T$  at lower temperatures reaching a maximum at  $\sim 40$  K. The magnitude of  $\mu_{\text{eff}}$  with increasing  $x$  to  $\sim 0.8\mu_B$  for  $x=0.37$  is in good agreement with the reported values of  $0.7\mu_B$  and  $T_{N2} \sim 40$  K obtained from neutron diffraction.<sup>8</sup>

We have performed Monte Carlo calculations of the effects of oxygen doping, which adds spins located at

formerly spinless Cu sites on the oxygen-deficient Cu planes. Frustration thereby introduced into the three-dimensional antiferromagnetic ordering leads to both excess  $\mu_{\text{eff}}$  at low temperatures and a reordering of the three-dimensional magnetic lattice. The effective moment determined from the Monte Carlo calculations increases, then decreases with  $x$  similar to the experimental observations. Magnetic susceptibility measurements of samples in the metallic regime,  $x \geq 0.5$ , show only a modest increase in  $\chi$  at low  $T$ . A composition-dependent Pauli susceptibility is observed, increasing approximately linearly with  $x$ , in contrast to early reports by Cava *et al.*<sup>19</sup> This increasing  $\chi^{\text{Pauli}}$  is consistent with decreasing local antiferromagnetic correlations with increasing  $x$ .

## II. EXPERIMENTAL TECHNIQUES

Powders of  $\text{YBa}_2\text{Cu}_3\text{O}_{6+x}$  where  $x$  varies from 0 to 1 were prepared as described previously.<sup>20</sup> To summarize briefly, samples of variable oxygen content were prepared under conditions of both low-temperature vacuum annealing and rapid quenching. Unless otherwise indicated, the susceptibility data reported here are for the rapidly quenched samples. In this procedure, pressed but unsintered pellets of  $\sim 500$  mg are equilibrated for 2 h in flowing air, nitrogen, or oxygen, at temperatures where the equilibrium oxygen content is known. These temperatures range from  $900^\circ\text{C}$  for  $x \leq 0.25$  to  $450^\circ\text{C}$  for  $x = 0.93$ . Samples were then quenched by direct immersion in liquid  $\text{N}_2$ . Oxygen contents were subsequently measured by thermal gravimetric analysis and shown to correspond with the values expected for equilibrium at the temperature from which the sample was quenched. The samples were determined to be single phase by x-ray diffraction and neutron diffraction. In particular, no magnetic  $\text{BaCuO}_2$  was evident from structural studies.

The magnetic susceptibility was measured on two previously described<sup>21</sup> Faraday susceptometers for temperatures of  $2 \leq T \leq 320$  K and magnetic fields up to 75 kG. The magnetic susceptibility data presented here have been corrected for core diamagnetism using  $-12$ ,  $-32$ ,  $-15$ , and  $-12 \times 10^{-6}$  emu per elemental mole of Y, Ba, Cu, and O, respectively.<sup>22</sup>

## III. EXPERIMENTAL RESULTS

The magnetic susceptibility of  $\text{YBa}_2\text{Cu}_3\text{O}_{6+x}$  as a function of temperature and oxygen content is summarized in Figs. 1 and 2 for oxygen content in the ranges of  $0.05 \leq x \leq 0.5$ , and  $0.5 \leq x \leq 1.0$ , respectively. Overall, the data are quite similar to the results of Johnston *et al.*<sup>3</sup> For samples of composition  $x = 1.0$ , the susceptibility is nearly temperature independent with the presence of a small increase at low temperatures. Analysis of the  $\text{YBa}_2\text{Cu}_3\text{O}_7$  sample data in terms of

$$\chi = \chi_0 + C_0/(T - \Theta) \quad (1)$$

gives a very good fit with  $\chi_0 = 2.84 \times 10^{-4}$  emu/mole  $\text{Cu}_3$ . We plot in the inset to Fig. 2  $(\chi - \chi_0)^{-1}$  vs  $T$  for this sam-

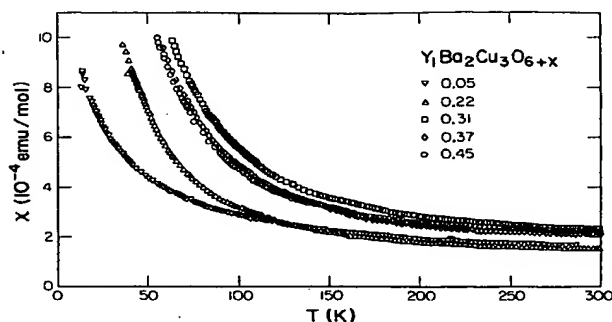


FIG. 1. Temperature-dependent magnetic susceptibility of  $\text{YBa}_2\text{Cu}_3\text{O}_{6+x}$  for  $0.0 \leq x \leq 0.5$ . The data have been corrected for core diamagnetism.

ple. The fit for  $C_0 = 2.14 \times 10^{-2}$  emu K/mole and  $\Theta = 19$  K suggests that the increase in the susceptibility at low temperature is due to the presence of  $1.9 \times 10^{-2}$  spin per Cu which may correspond to a magnetic impurity phase with a ferromagnetic  $\Theta = 19$  K as has been suggested in other work.<sup>23</sup> For compositions of smaller  $x$  a similar analysis is no longer appropriate. Use of Eq. (1) yields  $\Theta$  values other than 19 K for samples with  $0.5 \leq x \leq 0.8$ , and  $\chi_0$  terms no longer  $T$  independent. Hence, its application in this range of  $x$  is questionable, and the true behavior may be considerably more complex. For example, changing the annealing time at  $625^\circ\text{C}$  from 2 to 12 h gave a sample with the same oxygen stoichiometry,  $x = 0.65$ , the same value of  $\chi_0$ , but a Curie constant ( $C_0$ ) smaller by a factor of two. It is unlikely that these samples could contain sufficiently different impurity concentrations to rationalize this observation. Both  $\text{YBa}_2\text{Cu}_3\text{O}_{6.65}$  and  $\text{BaCuO}_2$ , the most likely impurity phase, should be stable and noninterconverting under these conditions.<sup>23,24</sup> In addition, nuclear quadrupole resonance (NQR)  $^{63}\text{Cu}$  studies as a function of decreasing oxygen content beginning with  $\text{YBa}_2\text{Cu}_3\text{O}_7$  suggest the presence of various Cu environments within the "metallic" sample.<sup>25</sup>

The semiconducting magnetic phase has a substantial increase in susceptibility as the temperature is decreased. Though it is tempting to attribute this rise as entirely due to impurities,<sup>6</sup> the systematic variation in the magnitude of the low-temperature susceptibility, combined with the absence of evidence for a magnetic impurity phase in the x-ray- and neutron-diffraction data supports the intrinsic nature of this phenomenon. The experimental susceptibility measured at 20 kG is presented as effective  $[p^{\text{expt}} = 2.83(\chi T)^{1/2}$  for  $\chi$  in emu/mol  $\text{YBa}_2\text{Cu}_3\text{O}_{6+x}$ ] versus  $T$  in Fig. 3. The  $p^{\text{expt}}$  has a maximum value at  $T \sim 40$  K. As oxygen content is increased ( $\chi - \chi_0$ ) from  $x = 0$ ,  $p^{\text{expt}}$  at 40 K increases, reaches a maximum for  $x \sim 3.5$ , then decreases (Fig. 4).

It is instructive to examine the room temperature susceptibility as a function of composition (Fig. 5). Qualitatively, the susceptibility appears to increase linearly with  $x$ , though for  $x > 0.5$  the susceptibility is nearly constant

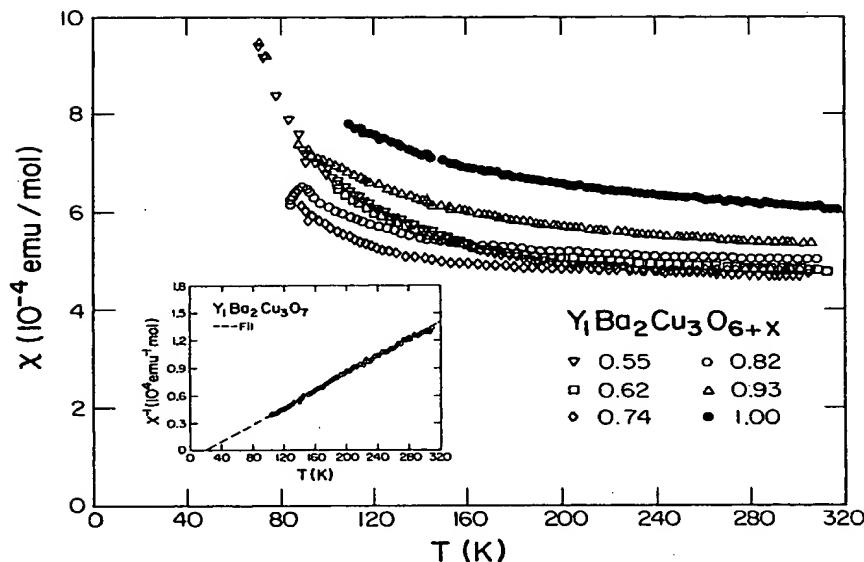


FIG. 2. Temperature-dependent magnetic susceptibility of  $\text{YBa}_2\text{Cu}_3\text{O}_{6+x}$  for  $0.5 \leq x \leq 1.00$ . The data have been corrected for core diamagnetism. Inset:  $(\chi - \chi_0)^{-1}$  vs  $T$  for  $x = 1.0$  (see text).

until  $x$  exceeds 0.8 (Fig. 6). An nuclear magnetic resonance (NMR)  $^{63}\text{Cu}$  study of the 300-K susceptibility as a function of composition for identically prepared samples confirm these results.<sup>25</sup>

#### IV. DISCUSSION

The magnetic properties of  $\text{YBa}_2\text{Cu}_3\text{O}_{6+x}$  for  $0 < x < 0.5$  can be understood by considering the spin frustration in the system. The unit cell consists of three layers of Cu sites, labeled in Fig. 7. For  $x = 0.0$ , neutron scattering experiments show that for the top ( $A, A'$ ) and bottom ( $C, C'$ ) layers all Cu sites are magnetic, while for the oxygen deficient central Cu ( $B, B'$ ) layer the Cu sites are non-magnetic, consistent with no holes in the system for this

value of  $x$ .<sup>4</sup> Within each magnetic layer ( $A, A', C, C'$ ), magnetic Cu sites are coupled two dimensionally by strong antiferromagnetic superexchange  $J$  which is the origin of the strong two-dimensional (2D) correlation similar to that seen in  $\text{La}_2\text{CuO}_4$ .

The scattering experiments further indicate that along the  $c$  axis, the top layer of one unit cell ( $A'$ ), and the bottom layer of the next unit cell ( $C$ ) are coupled antiferromagnetically through the Y sites, presumably by a direct exchange  $J_1$  between  $\text{Cu}^{2+}$ , since the O ions are

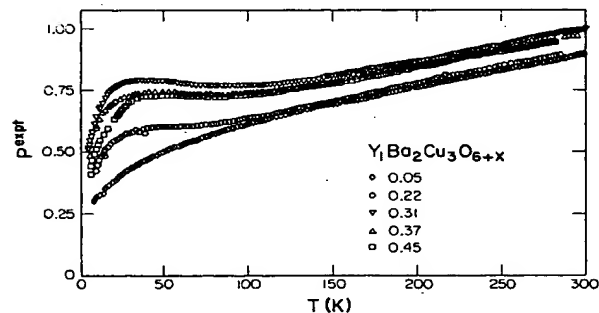


FIG. 3. Effective moment vs  $T$  for  $\text{YBa}_2\text{Cu}_3\text{O}_{6+x}$  and  $0.0 < x < 0.5$ .

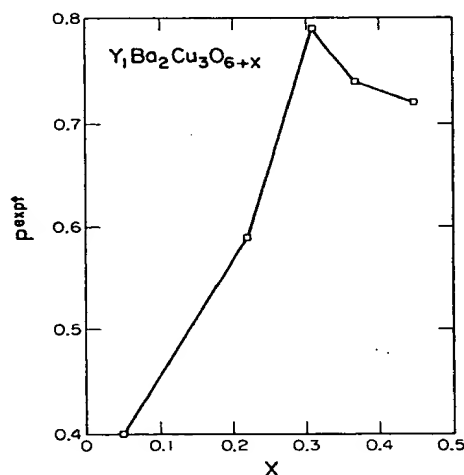


FIG. 4. Effective moment at 40 K vs  $x$  for  $\text{YBa}_2\text{Cu}_3\text{O}_{6+x}$  and  $0.0 < x < 0.5$ .

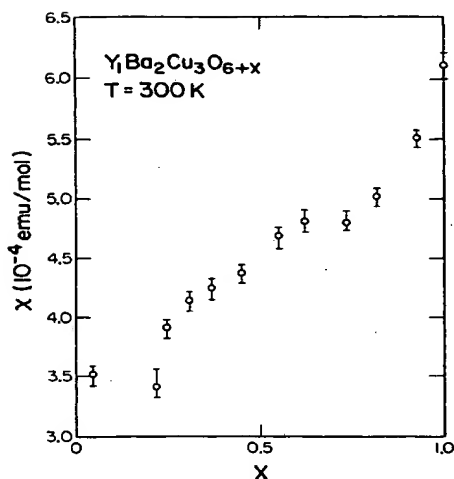


FIG. 5. Magnetic susceptibility at 300 K of  $\text{YBa}_2\text{Cu}_3\text{O}_{6+x}$  vs  $x$  for  $0.0 < x < 1.0$ .

missing around the Y sites. Within a unit cell, the top (*A*) and bottom (*C*) layers are coupled via the intervening O-deficient Cu layers (*B*). For  $x=0.0$ , when the Cu site on the central (*B*) plane is nonmagnetic, the *A* and *C* layers couple to each other antiferromagnetically (as indicated by the neutron scattering for  $x=0.0$  sample) through a weak superexchange  $J_2$  via  $\text{O}^{2-}$ , nonmagnetic Cu, and a second  $\text{O}^{2-}$ . This is type-I magnetic ordering below ordering temperature  $T_{N1}$ . However, when a Cu site on the *B* layer is magnetic, it couples to both the *A* and the *C* layers with a superexchange  $J_3$  analogous to the one in the *a-b* plane, hence larger than the antiferromagnetic superexchange  $J_2$  between the *A* and *C* layers just described. This is equivalent to coupling the *A* and *C* layers ferromagnetically. Thus whether the local coupling between the *A* and *C* layers within a unit cell is effective ferromagnetic (FM) or antiferromagnetic (AFM) is determined by

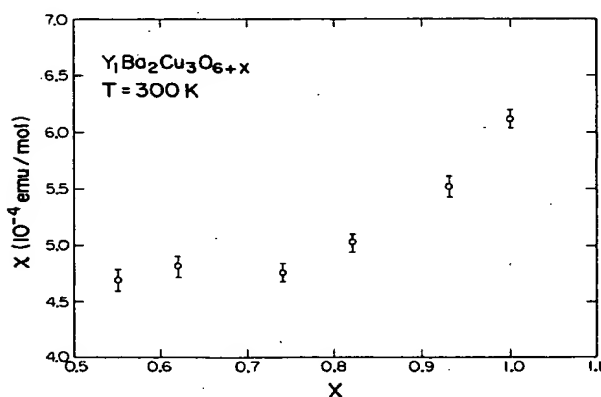


FIG. 6. Magnetic susceptibility at 300 K of  $\text{YBa}_2\text{Cu}_3\text{O}_{6+x}$  vs  $x$  for  $0.5 < x < 1.0$ .

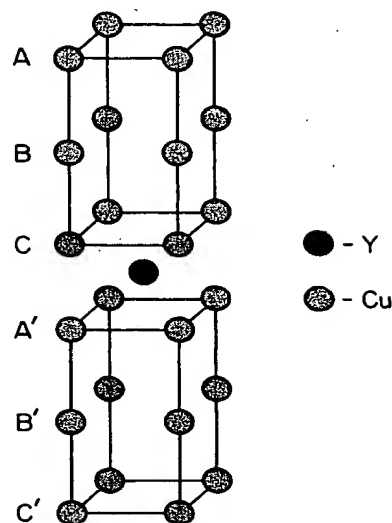


FIG. 7. Lattice structure of  $\text{YBa}_2\text{Cu}_3\text{O}_{6+x}$  showing Cu and Y sites. The figure shows O locations (solid lines) for  $x=0$ . For finite  $x$ , O atoms fill in sites between Cu in *B* and *B'* planes.

whether the *B* layer Cu site is magnetic or not. This competing FM and AFM coupling due to the interactions  $J_2$  and  $J_3$  is the origin of frustration in the system. At  $x=0$  the coupling of *A* and *C* is solely AFM (as long as no spins exist on the *B* layer), while as  $x$  increases the FM coupling increases producing frustration and a corresponding decrease in the Néel temperature.

There is not yet a consensus on how the oxidation states on the *A*, *B*, and *C* layers evolve with  $x$ .<sup>26</sup> Within our model, the spin concentration on each layer is determined by the number of holes produced by oxygen doping and their distribution among the *A*, *B*, and *C* layers.<sup>27</sup> Neutron-diffraction experiments indicate that there is an increase in the rate of addition of holes on the *A* and *C* layers per oxygen dopant as  $x$  increases beyond 0.4.<sup>28</sup> However, for simplicity we have used a linear variation of hole concentration on the *A*, *B*, and *C* layers with increasing  $x$ .

Monte Carlo simulations, based on this model of the couplings and oxygen valence evolution, have been carried out. The details are reported in Ref. 27. In the present case, we consider mainly the Ising model, since we have obtained qualitatively similar results in the *x-y* and Heisenberg versions of the model. The Ising model, plus the neglect of quantum fluctuations, overestimates the degree of 2D magnetic order within the *A* and *C* layers, and requires larger values of  $J_1$ ,  $J_2$ , and  $J_3$  ( $=0.2, 0.1$ , and  $0.4$  in units of  $J$ ) than expected from exchange integrals and experiment, but does not change the nature of the frustration introduced by oxygen doping. The values of the  $J$ 's were chosen so that, for hole concentrations of 40%, 20%, and 40% on the *A*, *B*, and *C* layers, respectively,  $T_N$  goes to zero near  $x=0.5$  and the predominate stable phase for small  $x$  is type I rather than type II.<sup>27</sup> Here we will give the following interpretation of the measured magnetic sus-

ceptibilities, using the results of simulations. For  $x$  close to 0.0, the  $A$  and  $C$  layers are strongly ordered within the  $a$ - $b$  plane and are coupled to each other antiferromagnetically, because most of the Cu sites on the central  $B$  layer are  $\text{Cu}^{1+}$  and nonmagnetic. This ordering throughout the entire lattice gives the broad antiferromagnetic peak for the susceptibility of the  $x=0$  materials above 300 K.<sup>3</sup> At this point the small number of magnetic  $\text{Cu}^{2+}$  on the central  $B$  layers are totally frustrated and behave like free spins, resulting in a small increase in susceptibility at low temperature. As  $x$  increases, filling in O vacancies on the  $B$  layer, more Cu sites on the  $B$  layer have spin, introducing frustration into the system. A new magnetic phase (type II) develops below  $T_{N2}$ , in which a finite moment appears on the  $B$  layer, inducing parallel ordering of the  $A$  and  $C$  layer spins. This doubling of the antiferromagnetic unit cell competes with the type-I order and the resulting frustration lowers both  $T_{N1}$  and  $T_{N2}$ . As  $x$  approaches 0.4 to 0.5, large numbers of holes enter the Cu  $A$  and  $C$  planes, associated with the metal-insulator transition, reducing the magnetic ordering within the plane and rapidly driving  $T_{N1}$  and  $T_{N2}$  to zero.<sup>6,29</sup> Thus, as  $x$  increases from 0.0 to 0.5, the contribution to the susceptibility of the AFM-ordered  $A$  and  $C$  layers becomes weaker and finally disappears, while the number of "free spins" on the  $B$  layer increases up to  $x \sim 0.3$ , resulting in an initial increase in the low temperature  $\chi$ . As  $x$  continues to increase beyond  $x \sim 0.3$ , the  $A$ - and  $C$ -layer antiferromagnetic order becomes weaker, and some spins on the  $B$ -layer order with the  $A$  and  $C$  layers, reducing the number of "free spins," and thus, the paramagnetic increase at low temperature.

Figure 8 presents the  $T$ -dependent susceptibility of the Ising model as a function of oxygen content. There is an initial drop of the Néel temperature with increasing oxygen content arising from frustration introduced by spins on the  $B$ -layer Cu sites. As  $x$  approaches 0.4, the second antiferromagnetic phase (type II) appears involving ordered spins on the chains. For  $x=0.5$  the antiferromagnetic transitions have broadened and disappeared. The results for  $x$ - $y$  Heisenberg models show a similar evolution

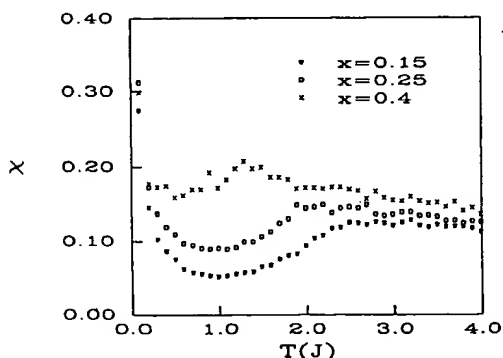


FIG. 8. Monte Carlo simulation of magnetic susceptibility per spin for Ising model representing  $\text{YBa}_2\text{Cu}_3\text{O}_{6+x}$ . The temperature is in units of the in plane AF exchange  $J$  and  $\chi$  is in units of  $\mu_B^2/J$ .

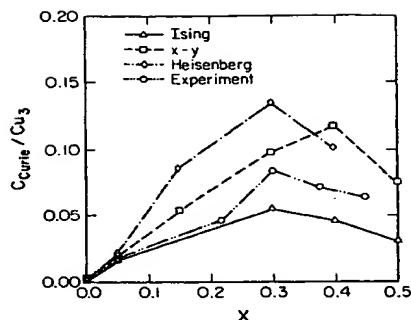


FIG. 9. Effective Curie constant obtained from Ising,  $x$ - $y$ , and Heisenberg models for the frustrated spin lattice together with experimental Curie constant obtained at 40 K.

as a function of  $x$  with the disappearance of long-range order occurring at somewhat lower  $x$ .<sup>27</sup>

The low temperature effective Curie constant goes through a maximum in the vicinity of  $x=0.3$  as  $x$  increases from 0.0 to 0.5. Figure 9 shows the results of the Monte Carlo calculations in the Ising  $x$ - $y$  and Heisenberg limits together with comparison to experimental results obtained at 40 K.<sup>27</sup> The maximum value of  $p^{\text{expt}}$  at 40 K is also in agreement with the effective moment associated with new magnetic order occurring at 40 K as detected by neutron diffraction.<sup>8</sup>

The variation of the measured susceptibility  $\chi(300 \text{ K})$  with  $x$  for  $x > 0.5$  is in contrast with the earlier reported results of Cava *et al.*<sup>19</sup> [Note that  $\chi(300 \text{ K})$  from Eq. (1), differs from  $\chi_0$  by only a small Curie contribution at  $T=300 \text{ K}$ .] We have not observed the sharply increased  $\chi$  at  $0.8 \geq x \geq 0.6$  reported in Ref. 19 in either the quenched or vacuum-annealed samples. For example, two samples of  $x=0.5$  prepared by quenching and annealing respectively show  $\chi(300 \text{ K})$  values that differ by less than 5%. In light of the increasing metallic nature of the  $\text{YBa}_2\text{Cu}_3\text{O}_{6+x}$  with increasing  $x$ , it is suggested that an increase in  $\chi_0$  for  $x > 0.8$  may be related to a reduction in the antiferromagnetic correlations with increasing  $x$ . It is noted that a constant value of  $\chi_0$  for  $0.55 \leq x \leq 0.74$  corresponds to a regime of constant  $T_c \approx 55 \text{ K}$ , while the regime of increasing  $\chi_0$  ( $x > 0.75$ ) corresponds to the transition to the stoichiometry range that gives the highest  $T_c \approx 90$ – $95 \text{ K}$ .

## V. SUMMARY

The temperature-dependent magnetic susceptibility of  $\text{YBa}_2\text{Cu}_3\text{O}_{6+x}$  varies smoothly with increasing  $x$  as the system varies from antiferromagnetic semiconductor to superconducting metal. For  $x < 0.5$  the susceptibility shows a concentration-dependent maximum in the effective moment at 40 K. This phenomenon is associated with the role of spin frustration and the onset of a second antiferromagnetic ordering at 40 K. The variation of magnetic susceptibility with temperature and composition in the metallic phase is suggestive of a reduced role for spin correlation with increasing  $x$  and an increase in susceptibility for highest  $T_c$ .

## ACKNOWLEDGMENTS

The authors acknowledge the assistance of Dr. S. Chittipeddi in obtaining neutron-diffraction data for samples used in this study, and Dr. R. K. Bordia in preparation of quenched samples. One of the authors (B.R.P.) would like to acknowledge support by the Air Force Office of Scientific Research and the Ohio Supercomputer Center.

- <sup>1</sup>J. G. Bednorz and K. A. Müller, *Z. Phys. B* **64**, 189 (1986).
- <sup>2</sup>M. K. Wu, J. R. Ashburn, C. J. Torng, P. H. Hor, R. L. Meng, L. Gao, Z. J. Huang, Y. Q. Wang, and C. W. Chu, *Phys. Rev. Lett.* **58**, 908 (1987).
- <sup>3</sup>D. C. Johnston, A. J. Jacobson, J. M. Newsam, J. T. Lewandowski, D. P. Goshorn, D. Xie, and W. B. Yelon, in *Chemistry of High Temperature Superconductors*, edited by D. L. Nelson, M. S. Whittingham, and T. F. George, ACS Symposium Series No. 351 (American Chemical Society, Washington, DC, 1987), p. 136.
- <sup>4</sup>J. M. Tranquada, D. E. Cox, W. Kunnmann, H. Moudden, G. Shirane, M. Suenaga, P. Zolliker, D. Vaknin, S. K. Sinha, M. S. Alvarez, A. J. Jacobson, and D. C. Johnston, *Phys. Rev. Lett.* **60**, 156 (1988).
- <sup>5</sup>A. J. Jacobson, J. M. Newsam, D. C. Johnston, D. P. Goshorn, J. T. Lewandowski, and M. S. Alvarez (unpublished).
- <sup>6</sup>J. M. Tranquada, A. H. Moudden, A. I. Goldman, P. Zolliker, D. E. Cox, G. Shirane, S. K. Sinha, D. Vaknin, D. C. Johnston, M. S. Alvarez, A. J. Jacobson, J. T. Lewandowski, and J. M. Newsam, *Phys. Rev. B* **38**, 2477 (1988).
- <sup>7</sup>W.-H. Li, J. W. Lynn, H. A. Mook, B. C. Sales, and Z. Fisk, *Phys. Rev. B* **37**, 9844 (1988).
- <sup>8</sup>(a) H. Kadowaki, M. Nishi, Y. Yamada, H. Takeya, H. Takei, S. M. Shapiro, and G. Shirane, *Phys. Rev. B* **37**, 7932 (1988); (b) M. Sato, S. Shamoto, J. M. Tranquada, G. Shirane, and B. Keimer, *Phys. Rev. Lett.* **61**, 1317 (1988).
- <sup>9</sup>The increased magnitude of the magnetic anomalies of the Nd system as compared with the  $\text{YBa}_2\text{Cu}_3\text{O}_{6+x}$  correlates with the even more anomalous behavior for the lighter rare-earth compounds containing Pr and Ce. For magnetic susceptibility studies, see S. Chittipeddi, Y. Song, D. L. Cox, J. R. Gaines, J. P. Golben, and A. J. Epstein, *Phys. Rev. B* **37**, 7454 (1988); S. Chittipeddi, Y. Song, J. P. Golben, D. L. Cox, J. R. Gaines, and A. J. Epstein (unpublished). For neutron-diffraction studies, see S. Chittipeddi, Y. Song, J. R. Gaines, W. E. Farneth, E. M. McCarron III, and A. J. Epstein, *J. Phys. (Paris) Colloq.* (to be published).
- <sup>10</sup>J. W. Lynn, W.-H. Li, H. A. Mook, B. C. Sales, and Z. Fisk, *Phys. Rev. Lett.* **60**, 2781 (1988).
- <sup>11</sup>P. W. Anderson, *Science* **235**, 1196 (1987); P. W. Anderson, G. Baskaran, Z. Zuo, and T. Hsu, *Phys. Rev. Lett.* **58**, 2790 (1987).
- <sup>12</sup>V. J. Emery, *Phys. Rev. Lett.* **58**, 2794 (1987).
- <sup>13</sup>P. A. Lee and M. Read, *Phys. Rev. Lett.* **58**, 2691 (1987).
- <sup>14</sup>J. E. Hirsch, *Phys. Rev. Lett.* **59**, 228 (1987).
- <sup>15</sup>S. A. Kivelson, D. S. Rokhsar, and J. P. Sethna, *Phys. Rev. B* **35**, 8865 (1987); S. Kivelson, *Phys. Rev. B* **36**, 8865 (1987).
- <sup>16</sup>D. J. Thouless, *Phys. Rev. B* **36**, 7187 (1987).
- <sup>17</sup>Y. Hasegawa and H. Fukayama, *Jpn. J. Appl. Phys.* **26**, L332 (1987).
- <sup>18</sup>J. R. Schrieffer, X.-G. Wen, and S.-C. Zhang, *Phys. Rev. Lett.* **60**, 944 (1988).
- <sup>19</sup>R. J. Cava, B. Batlogg, C. H. Chen, E. A. Rietman, S. M. Zahurak, and D. Werder, *Nature (London)* **329**, 423 (1987).
- <sup>20</sup>W. E. Farneth, R. K. Bordia, E. M. McCarron III, M. K. Crawford, and R. B. Flippin, *Solid State Commun.* **66**, 953 (1988).
- <sup>21</sup>F. Zuo, B. R. Patton, D. L. Cox, S. I. Lee, Y. Song, J. P. Golben, X. D. Chen, S. Y. Lee, Y. Cao, Y. Lu, J. R. Gaines, J. C. Garland, and A. J. Epstein, *Phys. Rev. B* **36**, 3603 (1987); S. Chittipeddi, Y. Song, D. L. Cox, J. R. Gaines, J. P. Golben, and A. J. Epstein, *Phys. Rev. B* **37**, 7454 (1988); J. S. Miller, D. A. Dixon, J. C. Calabrese, C. Vazquez, P. J. Krusic, M. D. Ward, R. L. Harlow, and E. Wasserman (unpublished).
- <sup>22</sup>L. N. Mulay and E. A. Boudreaux, *Theory and Applications of Molecular Diamagnetism* (Wiley, New York, 1986), p. 306.
- <sup>23</sup>S. S. P. Parkin, E. M. Engler, V. Y. Lee, and R. B. Beyers, *Phys. Rev. B* **37**, 131 (1988) report that  $\text{BaCuO}_2$  has a ferromagnetic  $\Theta$  of 19.0 K and  $\mu^{\text{eff}}$  of  $1.82\mu_B$ . We have synthesized a compound of composition  $\text{BaCuO}_2$  and have measured a ferromagnetic  $\Theta$  of 52.7 K and effective moment of  $1.71\mu_B$ . Hence, the identification of the composition of the apparent ferromagnetic impurity phase is uncertain.
- <sup>24</sup>Variations in the effective number of "impurity spins" with preparation conditions for samples of composition  $x > 0.5$  have been observed in earlier works. See, for example, Refs. 3, 19, and 23, T. Takabatake, M. Ishikawa, and T. Sugano, *Jpn. J. Appl. Phys.* **26**, L1859 (1987); D. C. Johnston, S. K. Sinha, A. J. Jacobson, and J. Newsam, *Physica B* (to be published); T. Kawagoe, T. Mizoguchi, K. Kanoda, T. Takahashi, M. Hasumi, and S. Kagoshima, *J. Phys. Soc. Jpn.* (to be published).
- <sup>25</sup>A. J. Vega, E. M. McCarron, and W. E. Farneth (unpublished).
- <sup>26</sup>Y. Tokura, J. B. Torrence, T. C. Huang, and A. I. Nazzari, *Phys. Rev. Lett.* **61**, 1127 (1988); M. Y. Su, S. E. Dorris, and T. O. Mason, *J. Solid State Chem.* **75**, 381 (1988).
- <sup>27</sup>Y. Lu and B. R. Patton (unpublished).
- <sup>28</sup>J. M. Tranquada, S. M. Heald, A. R. Moodenbaugh, and Y. Xu (unpublished).
- <sup>29</sup>H. Alloul, P. Mendels, G. Collin, and P. Monod, *Phys. Rev. Lett.* **61**, 746 (1988); S. I. Park, C. C. Tseui, and K. N. Tu, *Phys. Rev. B* **37**, 2305 (1988).

**CHRONOLOGICAL SCIENTIFIC for 2005**

Edit; National Astronomical Observatory of Japan

Publisher; MARUZEN Co., LTD

Date of publication; November 25, 2004

Physics 66 (412)

**MAGNETIC CHARACTERISTICS**

The quantity which represent the intensity of the magnetization of the substance is either the magnetic moment per unit volume  $M$  (unit: A/m) or  $P_M = \mu_0 M$  (unit: Wb/m<sup>2</sup> or T). These are respectively called magnetization intensity and magnetic polarization. In some cases,  $P_M$  is called magnetization intensity and is represented by  $M$ . The relation of these magnetization intensity with the two vector quantity representing a magnetic field, i.e.,  $B$  (magnetic flux density, unit: Wb/m<sup>2</sup> or T) and  $H$  (magnetic field intensity, unit: A/m), is expressed as  $B = \mu_0 (H + M) = \mu_0 H + P_M$ . According to the CGS electromagnetic unit system used in the field of magnetics (see "Physics 5"), the relation of  $B$  and  $H$  with magnetization intensity  $M_{CGS}$  is shown as  $B = H + 4\pi M_{CGS}$ . Though the unit of these quantities is same [cm<sup>-1/2</sup>g<sup>1/2</sup>s<sup>-1</sup>], they are respectively called G (gauss), Oe (oersted) and G (gauss). For converting into MKSA units, 1 G regarding magnetic flux density corresponds to 10<sup>-4</sup> T, 1 Oe regarding magnetic field corresponding to 10<sup>3</sup>/4 $\pi$  (79.577 to 80) A/m, and 1 G regarding magnetization corresponds to 10<sup>3</sup> A/m of  $M$  or 4 $\pi \times 10^{-4}$  T of  $P_M$ .

In common use, the intensity of the magnetization is often expressed as magnetic moment per unit mass (1g)  $\sigma_g$  ( $= M_{CGS}/$  (density in the CGS unit system)) or magnetic moment per mol  $\sigma_{mol}$  in the CGS electromagnetic unit system. The units of these quantity are often shown as G/g, emu/g, or G/mol, emu/mol.

In diamagnetic or paramagnetic substances,  $M$  is proportional to  $H$  unless  $H$  is extremely strong. The proportionality constant,  $\chi = M/H = P_M/\mu_0 H$ , is called magnetic susceptibility or susceptibility (or it may be called relative susceptibility if the magnetization intensity is shown by  $P_M$ ). The value of susceptibility in the CGS unit system  $\chi_{CGS} =$

$M_{CGS}/H$  is  $(1/4\pi)$  times  $\chi$  in the SI system. Practically, susceptibility per g or mol,  $\chi_{CGS,g} = \sigma_g/H$  or  $\chi_{CGS,mol} = \sigma_{mol}/H$  is often used. Units for these quantities are  $\text{cm}^3/\text{g}$  and  $\text{cm}^3/\text{mol}$  respectively, but they are often replaced with  $\text{emu/g}$  and  $\text{emu/mol}$ . In many paramagnetic substances, susceptibility changes depending on the temperatures and the behavior follows the Curie-Weiss' law, i.e.,  $\chi_{CGS,mol} = C_{mol}/(T-\Theta_p)$ .  $C_{mol}$  and  $\Theta_p$  are called Curie Constant and Asymptotic Curie Temperature respectively. On the other hand, the susceptibility of metal paramagnetic and diamagnetic substances is usually almost independent of temperatures.

In ferromagnetic substances, their magnetization  $M$  shows hysteresis and therefore  $M$  or  $B$  depends on not only the intensity of  $H$  but also how  $H$  was applied before. The condition of hysteresis is expressed by  $M$ - $H$  magnetization curves indicating the relationship of  $M$  and  $H$ , or  $B$ - $H$  magnetization curves indicating the relationship of  $B$  and  $H$ . The condition wherein  $M = 0$  at  $H = 0$  is called the demagnetization state, and a magnetization curve for increasing magnetic fields from this demagnetization state is called an initial magnetization curve. Initial magnetic permeability is  $1/\mu_0$ -times the inclination of  $B$ - $H$  initial magnetization curve in the vicinity of its origin, and is written as  $\mu_{ri}$ , while the maximum magnetic permeability is  $1/\mu_0$ -times the inclination of a tangential line drawn from origin to the  $B$ - $H$  magnetization curve, and is written as  $\mu_{max}$ . If the magnetic field increase, the intensity of magnetization comes close to a certain saturation magnetization  $M_s$ . Every ferromagnetic substance includes many divided sub-areas generally called magnetic domains, and in each magnetic domain, atoms' magnetic moment is aligned in a fixed direction. The intensity of magnetization caused by this phenomenon is called spontaneous magnetization. Practically, saturation magnetization is equal to spontaneous magnetization. The intensity of spontaneous magnetization is a quantity inherent in the substances, which reduces with temperature rise and becomes zero above the Curie Temperature  $T_c$ . This  $T_c$  is different from  $\Theta_p$  in both concept and actual value.

If applied magnetic field to a ferromagnetic substance is made to go and return in the range that exceed a positive and negative values of a magnetic field necessary for saturating the magnetization of the ferromagnetic substance, i.e. saturation magnetization field, the magnetization curve obtained will become closed curve. It is called a large hysteresis loop.

In the application of a ferromagnetic substance, the large hysteresis loop of  $B$ - $H$  magnetization curves is important. If the magnetic field is reduced after saturating the magnetization of a ferromagnetic substance, the magnetization changes via routes different from when the magnetic field is increased, and has finite magnetic flux density  $B_r$  (it may be called finite magnetization  $M_r$ ) even after the magnetic field became zero. This  $B_r$  is called residual magnetic flux density and the  $M_r$  is called residual magnetization. Further if the magnetic field is increased in the reverse direction, the magnetic flux density becomes zero when  $H = -B H_c$ . This  $B H_c$  is called coercive force. (Coercive force is sometimes defined, using the magnetic field  $M H_c$  where magnetization becomes zero on the  $M$ - $H$  magnetization curve). If the magnetic field strength in the reverse direction is more increased, it is finally saturated. Further when the direction of magnetic field strength change is here reversed again, ( $B, H$ ) or ( $M, H$ ) exhibiting the state of the ferromagnetic substance will make a round along the large hysteresis loop. The area  $W_h = \oint H dB$  (or  $(1/4\pi) \oint H dB$  in the CGS electromagnetic unit system) surrounded by the large hysteresis loop of  $B$ - $H$  magnetization curves represents the energy lost due to magnetic loss per AC magnetization cycle in the unit volume of a ferromagnetic substance. This is called a hysteresis loss. The  $B$ - $H$  magnetization curves, and  $B_r$ ,  $B H_c$  (or  $M H_c$ ),  $W_h$ ,  $\mu_{ri}$ ,  $\mu_{max}$ , etc. that characterize the  $B$ - $H$  magnetization curves are special characteristics varying according to substances. They can seriously change by additives, thermal treatments, processing, etc. Tables V and VI give examples of their typical values. It is generally desirable that  $B_r$  and  $B H_c$  are large in permanent magnet materials, and that  $\mu_{ri}$  and  $\mu_{max}$  are large, and  $B H_c$  and  $W_h$  are small, in the materials with high magnetic permeability used as the magnetic cores of transformers, etc.

12086

實・材料研究機構図書

2005.1.27

第50巻

50(43.4)

¥2,594

10167 2/24

2004

国立天文台 編

# 理科年表

机上版 第78冊

平成17年 2005



丸善株式会社

BEST AVAILABLE COPY

## 磁気的性質

物質の磁化の強さを表す量は単位体積当たりの磁気モーメント  $M$  (単位は  $A/m$ )、あるいは  $P_M = \mu_0 M$  (単位は  $Wb/m^2$ 、あるいは  $T$ ) である。それぞれを磁化の強さ、磁気極値という。場合によっては  $P_M$  を磁化の強さと呼び、記号  $M$  で表すこともある。これらと磁場を表す 2 つのベクトル量、 $B$  (磁束密度、単位  $Wb/m^2$ 、あるいは  $T$ ) と  $H$  (磁場の強さ、単位  $A/m$ ) の関係は、 $B = \mu_0 (H + M)$ 、 $M = \mu_0 H + P_M$  である。磁性的分野で用いられる CGS 電磁単位系 (物 5 参照) では、 $B$ 、 $H$  と磁化の強さ  $M_{CGS}$  の関係は  $B = H + 4\pi M_{CGS}$  である。これらの量の単位は同一  $[cm^{-1} g^{-1} s^{-1}]$  であるが、それぞれ  $G$  (ガウス)、 $Oe$  (エルステッド)、 $G$  (ガウス) と呼ぶ。MKSA 単位への換算は、磁束密度の  $1 G$  が  $10^{-4} T$ 、磁場の  $1 Oe$  が  $10^3 / 4\pi$  ( $79.577 \sim 80$ )  $A/m$  であり、磁化を表す量は  $1 G$  が  $M$  の  $10^3 A/m$ 、あるいは  $P_M$  の  $4\pi \times 10^{-4} T$  に相当する。

慣用として磁化の強さを、CGS 電磁単位系での単位質量 (1 g) 当たりの磁気モーメント  $\sigma_g (= M_{CGS} / (CGS \text{ 単位系での密度} \rho))$  あるいは物質 1 モル当たりの磁気モーメント  $\sigma_{mol}$  で表すことが多い。これらの量の単位をしばしば  $G/g$ 、 $emu/g$ 、あるいは  $G/mol$ 、 $emu/mol$  と記す。

反磁性体および常磁性体では、 $H$  が極めて強く限り  $M$  は  $H$  に比例する。この比例定数  $\chi = M/H = P_M/\mu_0 H$  を磁化率、あるいは帯磁率という ( $P_M$  で磁化の強さを表す場合には比磁化率ということがある)。CGS 単位系の磁化率  $\chi_{CGS} = M_{CGS}/H$  の数値は SI 系の  $\chi$  の  $(1/4\pi)$  倍である。また、実用上は、 $1 g$  あるいは 1 モル当たりの磁化率  $\chi_{CGS,g} = \sigma_g/H$ 、 $\chi_{CGS,mol} = \sigma_{mol}/H$  を用いることが多い。これらの量の単位はそれぞれ  $cm^3/g$ 、 $cm^3/mol$  であるが、これを  $emu/g$ 、 $emu/mol$  と書くことも多い。多くの常磁性体では、磁化率が温度変化し、キュリー・ワイスの法則  $\chi_{CGS,mol} = C_{mol}/(T - \theta_p)$  に従う。  $C_{mol}$ 、 $\theta_p$  をそれぞれキュリー定数、漸近キュリー温度という。一方、金属常磁性体や反磁性体の磁化率は通常ほとんど温度によらない。

強磁性体の磁化  $M$  はヒステリシス (履歴) 現象を示すので、 $M$  や  $B$  は  $H$  の大きさだけでなく、以前の  $H$  の印加の仕方にも依存する。その様子は、 $M$  と  $H$  の関係を表す  $M$ - $H$  磁化曲線、あるいは  $B$  と  $H$  の関係を表す  $B$ - $H$  磁化曲線によって表現される。  $H=0$  で  $M=0$  の状態を消磁状態といふ。この消磁状態から磁場を増加させるときの磁化曲線を初磁化曲線と呼ぶ。  $B$ - $H$  初磁化曲線の原点付近の傾きの  $1/\mu_0$  倍を  $\mu_{ri}$  と書き、これを初透磁率、また原点から  $B$ - $H$  磁化曲線の傾きの  $1/\mu_0$  倍を  $\mu_{max}$  と書き、これを最大透磁率という。磁場が大きくなると、磁化の強さは一定の飽和磁化  $M_s$  に近づく。強磁性体は一般に磁区と呼ばれる分域に分かれており、一つの磁区の中で原子の磁気モーメントは向きをそろえて整列している。このことによつて生じる磁化の強さを自発磁化という。実際上、飽和磁化は自発磁化と等しい。自発磁化の強さは物質固有の量であり、温度の上昇とともに減少して、キュリー温度  $T_c$  以上でゼロになる。この  $T_c$  は概念上も、実際の値も  $\theta_p$  とは異なる量である。

強磁性体の磁化を飽和させるのに必要な磁場 (飽和磁場) 以上の磁場を正の値と負の値の間で往復させると、磁化曲線は閉曲線となる。これを大ヒステリシスループという。強磁性体の応用では、 $B$ - $H$  磁化曲線の大ヒステリシスループが重要である。強磁性体の磁化を飽和させた後、磁場を減少させると、

磁化は磁場の増加のときと異なる経路をたどって変化し、磁場がゼロになつても、有限の磁束密度  $B_r$  (有限の磁化  $M_r$  を持つ) を持つ。この  $B_r$  を残留磁束密度、 $M_r$  を残留磁化という。さらに逆方向に磁場を増加させると、 $H = -B_r/\mu_0$  で磁束密度がゼロとなる。この  $B_r$  を保磁力という ( $M$ - $H$  磁化曲線上で磁化がゼロとなる磁場  $H_r$  で保磁力を定義することもある)。さらに逆方向の磁場の強さを増加すると、ついに逆方向の飽和に達する。ここで再び磁場の変化の方向を逆転すれば、強磁性体の状態を示す ( $B$ ,  $H$ ) あるいは ( $M$ ,  $H$ ) は大ヒステリシスループに沿って一周する。  $B$ - $H$  磁化曲線の大ヒステリシスループの囲む面積  $W_M = \oint H dB$  (CGS 電磁単位系では  $(1/4\pi) \oint H dB$ ) は、強磁性体の単位体積中で、交流磁化 1 サイクルの間に磁気的な損失によつて失われるエネルギーである。これをヒステリシス損失という。  $B$ - $H$  磁化曲線、およびそれ特徴づける  $B_r$ ,  $H_r$  (あるいは  $M_r$ ,  $H_r$ )、 $\mu_{ri}$ ,  $\mu_{max}$  等は、材料によつて異なる特性であつて、添加物、熱処理、加工等によつて大きく変わる。表 V, VI では代表的な値の一例を掲げる。一般に永久磁石材料では  $B_r$  と  $H_r$  が大きいことが、またトランスの磁心等に用いる高透磁率材料では、 $\mu_{ri}$  や  $\mu_{max}$  が大きく、 $B_r$  と  $H_r$  が小さいことが望ましい。

## I. 常磁性イオン

常磁性イオンを含む常磁性体のキュリー定数は  $C_{mol} = N\mu_B^2/3k_B$  で与えられる。  $N$  は 1 モル中の常磁性イオンの個数である。  $\mu_B$  は有効ボーア磁子数で、磁性イオンの電子状態によつて決まる。

## 鉄族イオン

イオン	3d 電子数	自由イオン項	$\rho$ (計算)	$\rho$ (実験)
Ti <sup>3+</sup> , V <sup>4+</sup>	1	<sup>2</sup> D <sub>3/2</sub>	1.73	1.7-1.9
V <sup>3+</sup>	2	<sup>3</sup> F <sub>2</sub>	2.83	2.7-2.9
Cr <sup>3+</sup> , V <sup>2+</sup>	3	<sup>4</sup> F <sub>3/2</sub>	3.87	3.8-3.9
Mn <sup>3+</sup>	4	<sup>6</sup> D <sub>5/2</sub>	4.90	4.8-4.9
Mn <sup>2+</sup> , Fe <sup>3+</sup>	5	<sup>6</sup> S <sub>5/2</sub>	5.92	5.8-5.9
Fe <sup>2+</sup>	6	<sup>5</sup> D <sub>4</sub>	4.90	5.2-5.5
Co <sup>3+</sup>	7	<sup>3</sup> F <sub>4</sub>	3.87	4.8-5.1
Ni <sup>2+</sup>	8	<sup>3</sup> F <sub>4</sub>	2.83	2.8-3.3
Cu <sup>2+</sup>	9	<sup>1</sup> D <sub>3/2</sub>	1.73	1.8-2.0

## 希土類イオン

イオン	4f 電子数	自由イオン項	$\rho$ (計算)	$\rho$ (実験)
Ce <sup>3+</sup>	1	<sup>2</sup> F <sub>5/2</sub>	2.54	2.4
Pr <sup>3+</sup>	2	<sup>3</sup> H <sub>4</sub>	3.58	3.5
Nd <sup>3+</sup>	3	<sup>4</sup> F <sub>3/2</sub>	3.62	3.5
Pm <sup>3+</sup>	4	<sup>5</sup> I <sub>6</sub>	2.68	
Sm <sup>3+</sup>	5	<sup>6</sup> H <sub>5/2</sub>	1.55*	1.5
Eu <sup>3+</sup>	6	<sup>7</sup> F <sub>0</sub>	3.40*	3.4
Gd <sup>3+</sup>	7	<sup>8</sup> S <sub>7/2</sub>	7.94	8.0
Tb <sup>3+</sup>	8	<sup>7</sup> F <sub>6</sub>	9.72	9.5
Dy <sup>3+</sup>	9	<sup>6</sup> H <sub>15/2</sub>	10.65	10.6
Ho <sup>3+</sup>	10	<sup>5</sup> I <sub>6</sub>	10.61	10.4
Er <sup>3+</sup>	11	<sup>4</sup> I <sub>15/2</sub>	9.58	9.5
Tm <sup>3+</sup>	12	<sup>3</sup> H <sub>6</sub>	7.56	7.3
Yb <sup>3+</sup>	13	<sup>2</sup> F <sub>7/2</sub>	4.54	4.5

\* Van Vleck-Frank の理論による値。

$$g = \frac{3}{2} + \frac{S(S+1) - L(L+1)}{2J(J+1)}$$

その他の記号は物 18 参照。